BUNDESREPUBLIK
DEUTSCHLAND

Bundesanstalt für
Geowissenschaften und
Rohstoffe (BGR)

Hannover

REPÚBLICA DE HONDURAS

Empresa Nacional de
Energía Eléctrica (ENEE) –
Empresa de Generación

Tegucigalpa

Regional Project
Geothermal Energy Central America

Lineament Mapping in Namasigüe/El Trifuno (Choluteca, Honduras) based on Remote Sensing data

Alina Ermertz
Dr. Kai Hahne

Hannover, May 2019

Lineament Mapping in Namasigüe/El Trifuno (Choluteca, Honduras) based on Remote Sensing data

Authors	Alina Ermertz (BGR)
	Dr. Kai Hahne (BGR)

Project Number	2014.2508.1
BGR Number	05-2391
Project Partner	Empresa Nacional de Energía Eléctrica (ENEE) – Empresa de Generación
Pages	32
Place and date of issuance	Hannover, May 2019

Table of Contents

Abbreviations

BGR	Bundesanstalt für Geowissenschaften und Rohstoffe (Federal Institute for Geosciences and Natural Resources)
DEM	Digital Elevation Model
ENEE	Empresa Nacional de Energía Eléctrica
GIS	Geographic Information System
GPS	Global Positioning System
m asl	Metres above sea level
MSI	MultiSpectral Instrument
RGB	Red Green Blue (colour band combination)
SRTM	Shuttle Radar Topography Mission
UAV	Unmanned Aerial Vehicle
UNAH	Universidad Nacional Autónoma de Honduras
WP	Waypoint (Measured by GPS)

List of figures

In figures, that show field photos, the location refers to a GPS waypoint (WP). All waypoints are listed in a table and a corresponding map in the appendix to allow traceability of the field survey.

Summary

Within the regional project of Technical Cooperation “Identification of Geothermal Resources in Central America”, a workshop was conducted with the partner ENEE in February 2019 in Honduras. The focus was set on the use of remote sensing data for geothermal exploration. Furthermore, four days of field work for a general overview as well as an inspection of geothermal manifestations and local tectonics was conducted jointly.

The two study areas Namasigüe and El Trifuno in southern Honduras are objects of this study. Multispectral satellite imagery (Sentinel-2) and digital elevation models (SRTM) were used for the structural analysis. Lineaments are the expression of faults on the earth’s surface and indicate areas with high permeability for hydrothermal fluids. The aim of a lineament mapping in this case study is to define areas of increased geothermal potential, appropriate for further exploration.

The tectonic setting of southern Honduras is controlled by the North American-Caribbean plate boundary in the north and the Cocos-Caribbean convergent plate boundary in the southwest. Major fault systems occur throughout the country and strike in NW, NE and N-S directions that can be detected on a regional scale in the study areas as well. Additionally, numerous shear lenses that developed along NE-oriented transtensional faults characterise the working areas.

Results of the lineament analysis suggest further investigations in the southwestern part of the study areas, where topography is low and a dense network of lineaments occurs. NE-oriented faults seem to be the most active and manifestations for geothermal activity may preferably occur along these structures. The integration of UAV surveys is also recommended for a fast and more detailed area-wide exploration.

1 Scope of the Work

The regional project “Technical Cooperation Geothermal Energy in Central America” includes cooperation with the partner agency Empresa Nacional de Energía Eléctrica (ENEE), specifically the Empresa de Generación, in Honduras. So far, the only geothermal plant producing energy in Honduras since 2017 has been GeoPlatanares. The government is interested in extending the geothermal sector in order to reduce the dependency on the problematic hydropower sector and fossil fuel imports with a stable energy resource, which is why ENEE focusses on extending the exploration of areas with high geothermal potential. Such studies are planned in cooperation with a team from the University of Honduras (Universidad Nacional Autónoma de Honduras, UNAH), who is using such investigation possibilities for qualifying the geothermal exploration topic in relevant careers. Remote sensing as an area-wide, fast and cost-efficient technique is part of this exploration and used for tectonic studies. The identification of faults and lineaments is important for the definition of areas with high permeability acting as pathways for hydrothermal fluids.

Multispectral data from the Sentinel satellite mission and elevation data from the SRTM mission form the basis for a structural analysis of the exploration area Namasigüe/El Trifuno in the region of Choluteca near the Nicaraguan border.

A first field check has been conducted together with the partners of ENEE and UNAH from 15/02/2019 to 19/02/2019.

2 Working Areas

The working areas are located in southern Honduras in the department of Choluteca near the Nicaraguan border. Two study areas were defined by ENEE, Namasigüe covering ca. 217 km² and El Trifuno encompassing ca. 307 km² (Figure 2.1).

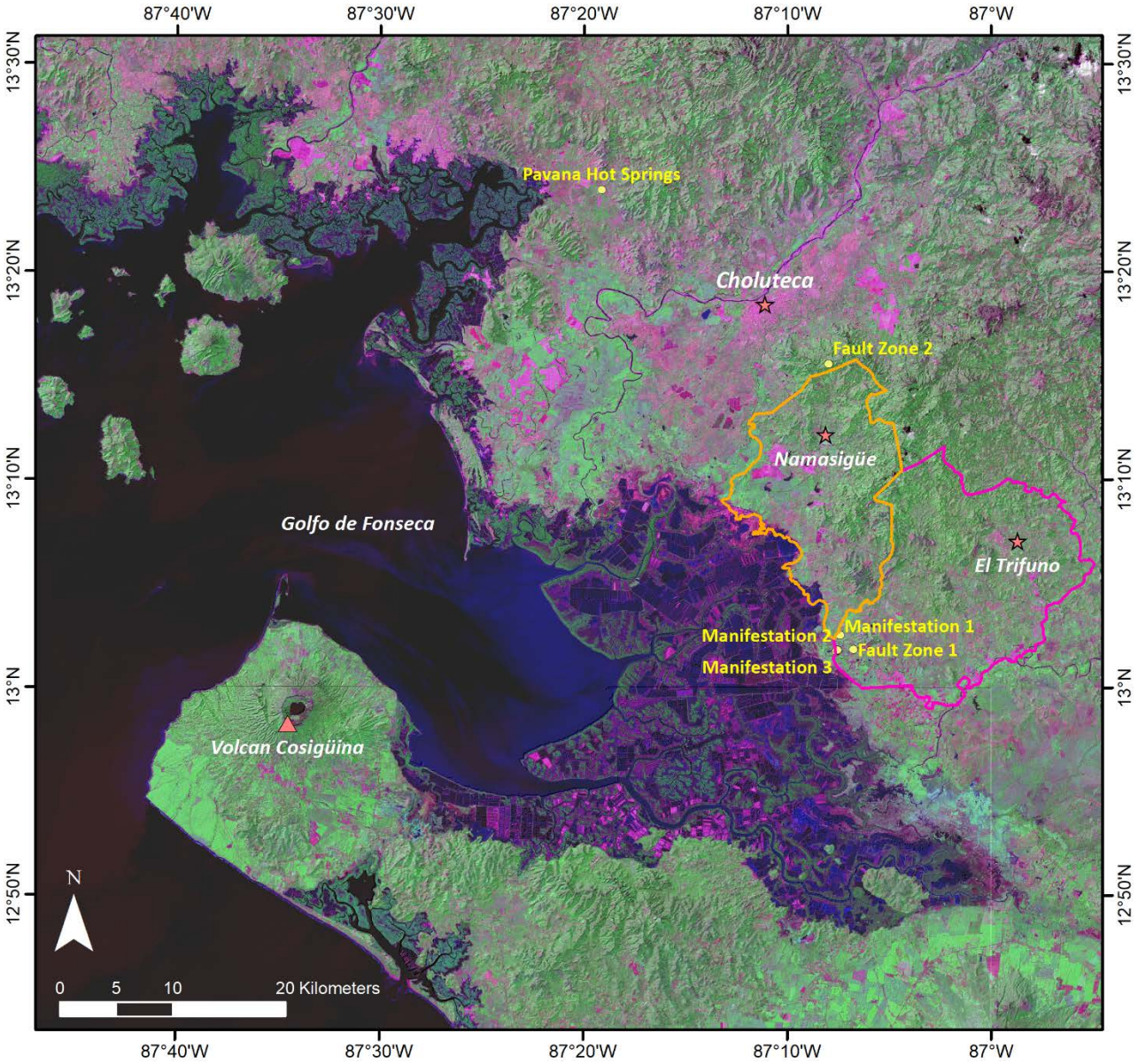

Figure 2.1: Working areas in southern Honduras: Namasigüe (orange) and El Trifuno (red). Displayed on Sentinel 2A, bands 12-8a-5 (RGB) and SRTM shaded relief. The yellow labels are visited points.

3 Remote Sensing Data

The following data is implemented in Quantum GIS (version 3.4.4) for further analysis and lineament vectorization:

- Enhanced and geocoded satellite images and DEMs (using ENVI for e.g. high pass filtering, histogram stretching, shaded relief generation):
    - Sentinel 2A MSI acquired November, 13, 2018; 20 m ground resolution.

Band number	Central wavelength (nm)	Bandwidth (nm)	Spatial resolution (m)
1	443	20	60
2	490	65	10
3	560	35	10
4	665	30	10
5	705	15	20
6	740	15	20
7	783	20	20
8	842	115	10
8b	865	20	20
9	945	20	60
10	1380	30	60
11	1610	90	20
12	2190	180	20

Figure 3.1: Band characteristics of Sentinel-2 MSI (ESA 2012).

    - RapidEye for Namasigüe; 5 m ground resolution.
    - SRTM 30 m digital elevation model,
- Information from overview-field work (4 days only):
    - Shape and visibility of lineaments,
    - Additional geological and tectonic information,
    - Field photos,
    - Waypoints (WP) GPS measurements of findings and locations of photos.

The spatial reference system used for this study is UTM 16 N, WGS 84.

The following thematic layers have been created:

- Shaded relief maps
- Enhanced Sentinel 2A multispectral images

- Waypoints with corresponding data tables concerning information from fieldwork (manifestations, lithology, photos etc.).
- Faults, large-scale
- Faults, small-scale
- Exploration area

Additional field photos- not mentioned in this report- and their locations, are attached on DVD to this report, designed as a Quantum GIS-project.

4 Geology & Plate Tectonic Setting

Central America represents the connection between the North American and South American continents, separating the Caribbean Sea in the east from the Pacific Ocean in the west. The geologic history of this area is characterized by a complex interaction of different tectonic plates, the North and South American, Cocos, Nazca and the Caribbean Plate, related volcanism and continental block rotation (Bundschuh et al. 2007; James 2007; Mann 2007).

4.1 Geologic History

The Central American complex exists of Precambrian-Paleozoic continental terranes that accreted to form the Chortis block by Late Cretaceous times (Mann 2007; Rogers et al. 2007). The boundaries of these terranes nowadays strike perpendicular to the Central American volcanic chain and may have been an important factor influencing the formation of tectonic structures during the Cocos-Caribbean subduction history (Mann 2007). To the north, large strike-slip faults of the Motagua fault zone represent the boundary between the Chortis and the Maya block, also corresponding to the boundary between the Caribbean and the North American plate (James 2007; Figure 4.1).

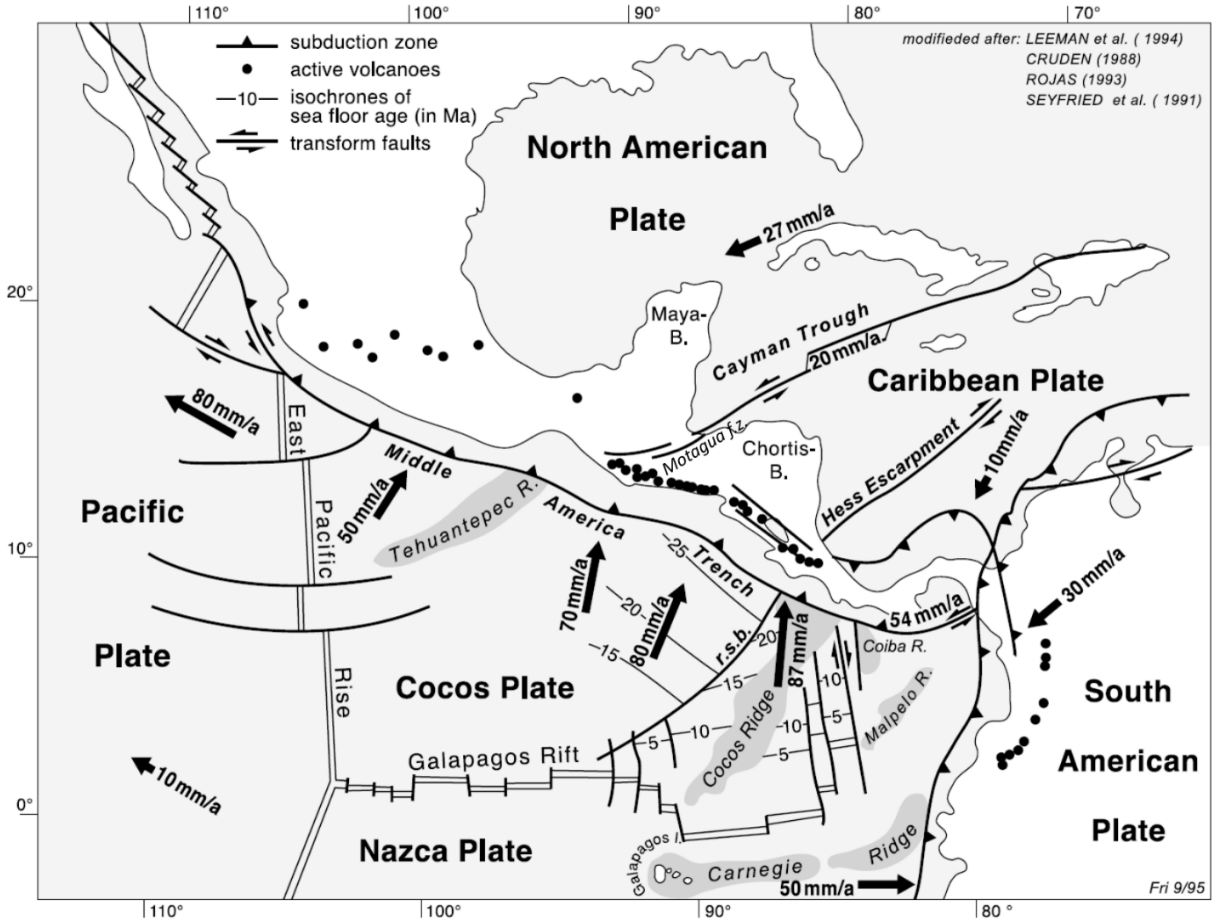

Figure 4.1: Regional geological setting of Central America (after Frischbutter 2002). The chain of active volcanoes extends from the Mexican-Guatemala border to central Costa Rica.

The basement rocks of Honduras are also part of the Chortis block and are represented by Paleozoic low-grade metamorphic rocks (Eppler et al. 1986). In the area of northwestern Nicaragua, the metamorphic basement is termed *Nueva Segovia Schist*, named after the department Nueva Segovia where most of the outcrops occur (Ortega-Gutierrez et al. 2007). Rocks of this complex consist of schists, phyllites, marbles, quartzites and gneisses intensely folded and penetrated by quartz veins and pods (Ortega-Gutierrez et al. 2007). These rocks occur close to the Honduran border to the northeast of Choluteca, observed at one location southeast of Choluteca along the track from WP 016 to WP 025.

There is no record of sedimentary or volcanic rocks of proven Paleozoic age, indicating that the metamorphic basement is overlain by Mesozoic sediments (Eppler et al. 1986; Ortega-Gutierrez et al. 2007). In particular, this Mesozoic cover consists of low-grade Upper Triassic to Middle Jurassic metasediments overlain by Lower Cretaceous clastic and carbonate platform deposits and Upper Cretaceous redbeds (Eppler et al. 1986; Ortega-Gutierrez et al. 2007).

The youngest rocks of the area are volcanic sequences of Tertiary age (Eppler et al. 1986). Active volcanism is absent and therefore not the heat source for geothermal systems, although the large amount of manifestations indicates geothermal potential. Geothermal sites are therefore bound to tectonic structures (Eppler et al. 1986; Heiken et al. 1991).

4.2 Tectonics

Main tectonic components controlling the Central American region are the Caribbean-North American plate boundary in northern Honduras and Guatemala and the convergent Cocos-Caribbean plate boundary in the southern segment of the Middle American Trench (Figure 4.1).

The Caribbean-North American plate boundary is represented by an oceanic basin, the Cayman Trough, offshore and by the Motagua fault onshore (Mann 2007; Figure 4.1). The Motagua fault zone is a ca. 400 km long and 80 km wide complex of sinistral strike-slip faults, roughly striking E-W with a concave trend towards the north (James 2007; Ortega-Gutierrez et al. 2007; Ratschbacher et al. 2009).

To the southwest of the Chortis block, the Cocos plate subducts beneath the Caribbean plate in the northeasterly direction (Figure 4.1). The Cocos-Caribbean assembly is a segment of the Middle American subduction zone with increasing convergence rates towards the southeast (DeMets 2001; Figure 4.1) generating counterclockwise rotation of tectonic blocks accommodated by movement along major strike-slip faults (Burkart & Self 1985).

Cocos-Caribbean subduction processes result in active tectonics and volcanic activity with more than 40 volcanic centers from the Mexican-Guatemala border to central Costa Rica (Bundschuh et al. 2007). The Nicaraguan depression is a structure that characterizes the Pacific Coast extending

over 600 km parallel to the volcanic arc. Because major volcanoes are being located within the Nicaraguan depression and not to its southwest, the structure is interpreted as an intra-arc basin rather than a back-arc basin (Funk et al. 2009). It is mostly described as a half-graben structure that formed in a Plio- to Pleistocene extensional phase and extends parallel to the Middle American Trench from El Salvador to Costa Rica (Marshall 2007).

The tectonic history can mainly be divided into three tectonic phases. The first phase occurred as a convergent deformation phase in Miocene times where NW-trending structures developed, followed by a NE-SW orientated Pliocene extensional phase. The third deformation phase is transtensional and still ongoing since the early Pleistocene (Weinberg 1992). Present-day movement along the coast most likely follows right-lateral movement along the NW-striking Nicaraguan depression, which itself is bounded to its southwest by NW-striking transtensional strike-slip faults (Weinberg 1992). There are different models to explain the complex pattern of differently striking faults and the ongoing transtensional phase along the coast (Funk et al. 2009).

The transform fault model explains the offsets that are evident within the Central American volcanic arc with a series of transform faults. A second model suggests pull-apart structures bounded by transform faults as the result of extension forced by right-lateral movement between a forearc sliver and the continent (Funk et al. 2009). The bookshelf fault model explains the general dextral movement along the coast to be accommodated by N30°-45°E-striking sinistral faults including a clockwise rotation of crustal blocks that implicates the movement of the forearc sliver (La Femina et al. 2002).

4.3 Geothermal energy in Honduras

Studies for the investigation of geothermal potential in Honduras have been conducted since the late 1970 (Eppler et al. 1986). Different sites in Honduras were evaluated considering their potential for further development as sources for electrical power (Eppler et al. 1986; Heiken et al. 1991). The site with the greatest potential and highest reservoir temperatures of 225°-240°C, Platanares, is located in western Honduras and has been operating as the first geothermal power plant (GeoPlatanares) in Honduras since 2017. Most of the manifestations lie within a large, up to 1 km wide, NW-trending fault zone (Heiken et al. 1991). Hot springs are the result of the deep circulation of meteoric waters along Neogene faults of a system described as similar to the Basin and Range type in the United States, characterized by thin crust and high regional heat flow (Eppler et al. 1986; Heiken et al. 1991).

In 1985, Los Alamos National Laboratory conducted hydrogeochemical studies in six different hydrothermal systems in western Honduras. As the samples of the Namasigüe area are the only samples that exhibit a volcanic influence, this area attracts special interest for further investigations.

5 Tectonic Structures in the Working Areas

The structural setting of Honduras is mainly controlled by the above-mentioned plate boundaries, the Caribbean-Cocos boundary in the southwest and the Caribbean-North American boundary in the north, and the directions of faults follow these controlling factors.

The longest continuous fault complex in Honduras is the Guayape fault system, which extends at least 290 km from the Caribbean Coast south-westwards to the Nicaraguan border and possibly continues to the Gulf de Fonseca reaching the above mentioned project areas (Finch & Ritchie 1991). This system exhibits a general NE-oriented trend with a fault zone of up to 25 km width, representing one of the dominant structural trends (Finch & Ritchie 1991; James 2007; Figure 5.1).

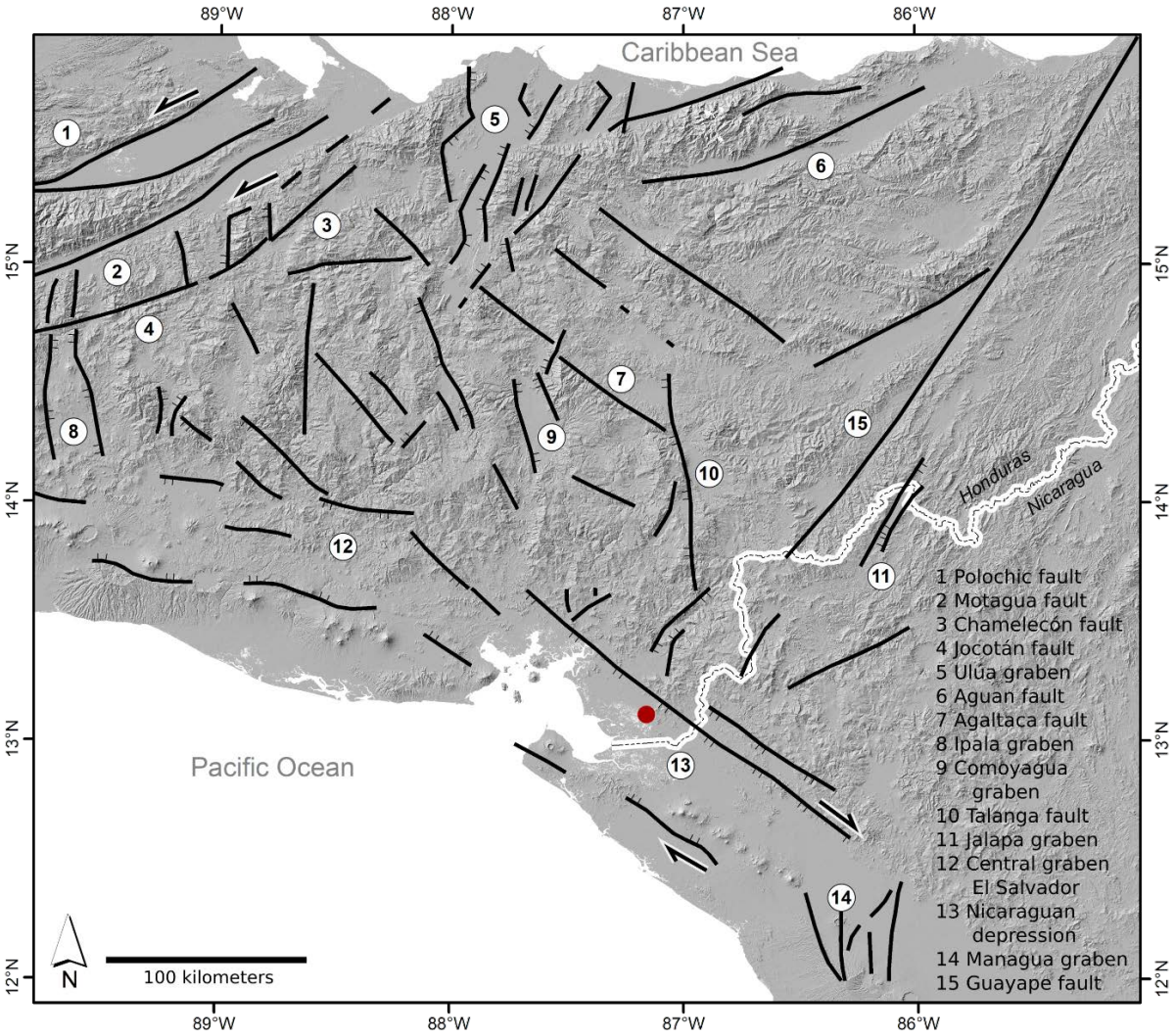

Figure 5.1: Major fault systems of the northern Chortis block (modified after James 2007). The red point indicates the location of the study areas. Structures dominantly strike NW-SE like the Nicaraguan depression (13), NE-SW like the Guayape fault system (15) and N-S like a series of graben systems (5, 8, and 9).

Other major structural directions are represented by N-S oriented graben systems as well as by NW-trending faults paralleling the Pacific Coast and therefore the Middle American Trench

(James 2007; Weinberg 1992; Figure 4.1). These trends are also visible in the volcanic chain, that by itself is oriented NW-SE with displacements in a NNW-SSE striking direction (Figure 5.2).

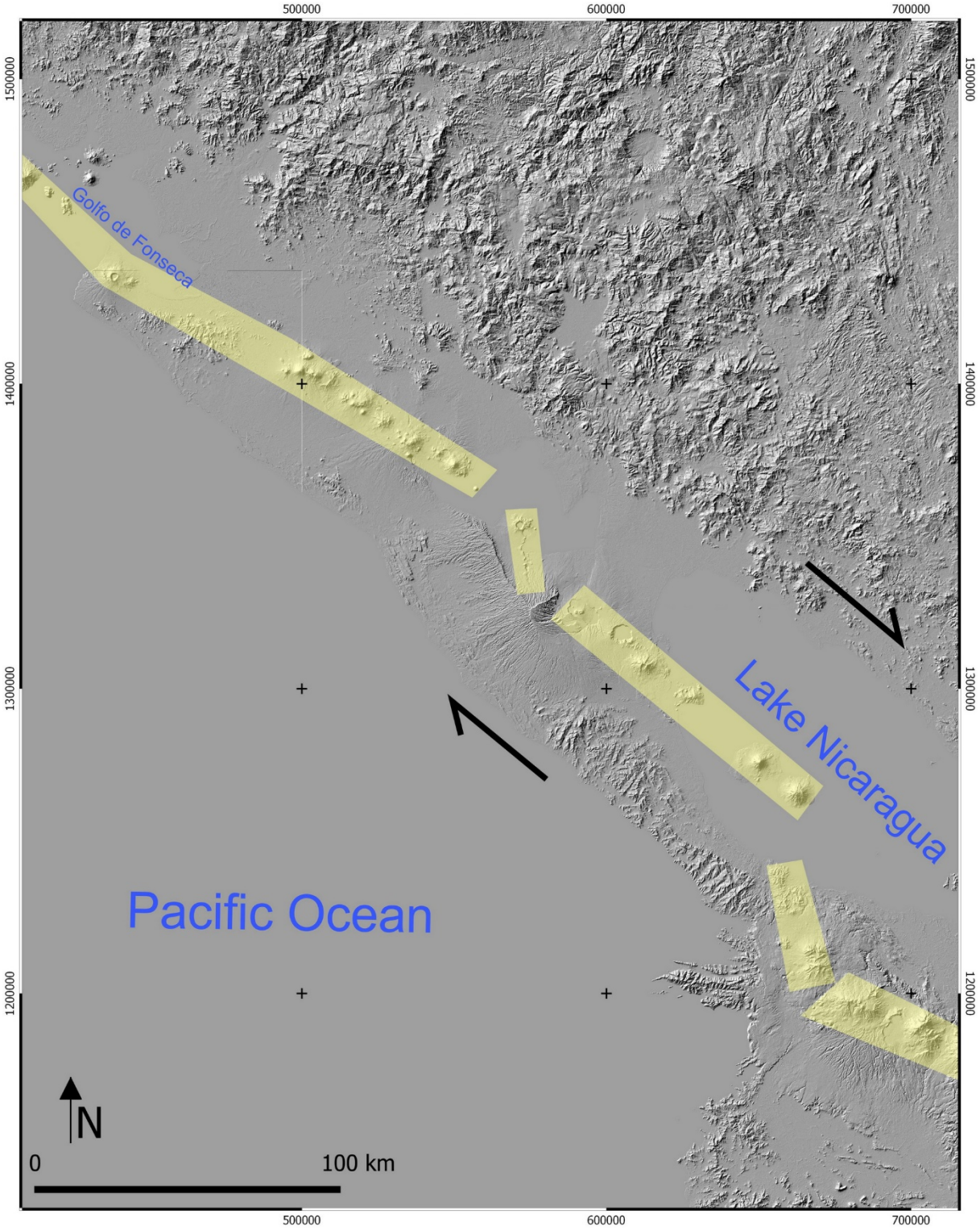

Figure 5.2: The main volcanic chain of the Nicaraguan depression (see also fig. 5.1) and its displacements (highlighted by yellow polygons) due to transversal faulting superimposed on shaded relief SRTM DEM.

5.1 Structural Analyses

The structural analyses were conducted with enhanced multispectral satellite images and shaded relief DEMs with different illumination angles. By using these combinations, it was possible to detect structures also in areas of low topography (Figures 5.9 – 5.12).

All major fault directions (NW-SE; N-S; NE-SW) described in the literature are also visible in the remote sensing data, especially on a regional scale (Figures 5.4, 5.5).

The closer view reveals numerous shear lenses, which have developed mainly along NE-oriented transtensional faults (Figures 5.6, 5.7 and 5.9 – 5.12). They can be considered as a result of the transtensional northeastern movement of the Chortis Block in accordance to the Guayape fault system (Figure 5.1). Most of these transtensional faults within the working areas show a right lateral sense of shearing (Figure 5.8).

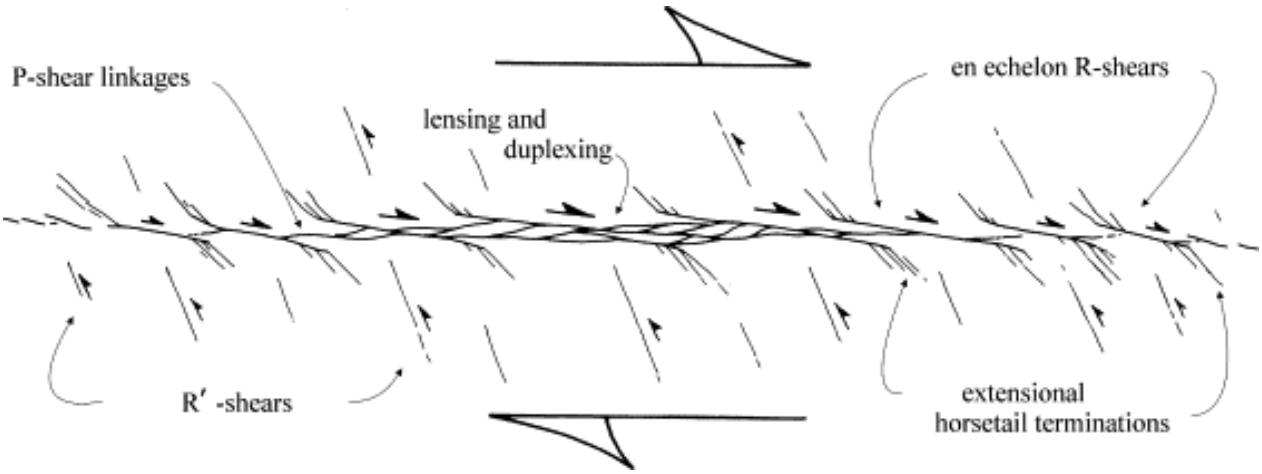

Figure 5.3: Fault zone terminology (Swanson 2006). The lensing and duplexing creates anastomosing patterns and illustrates the situation in the working areas especially in a large-scale view.

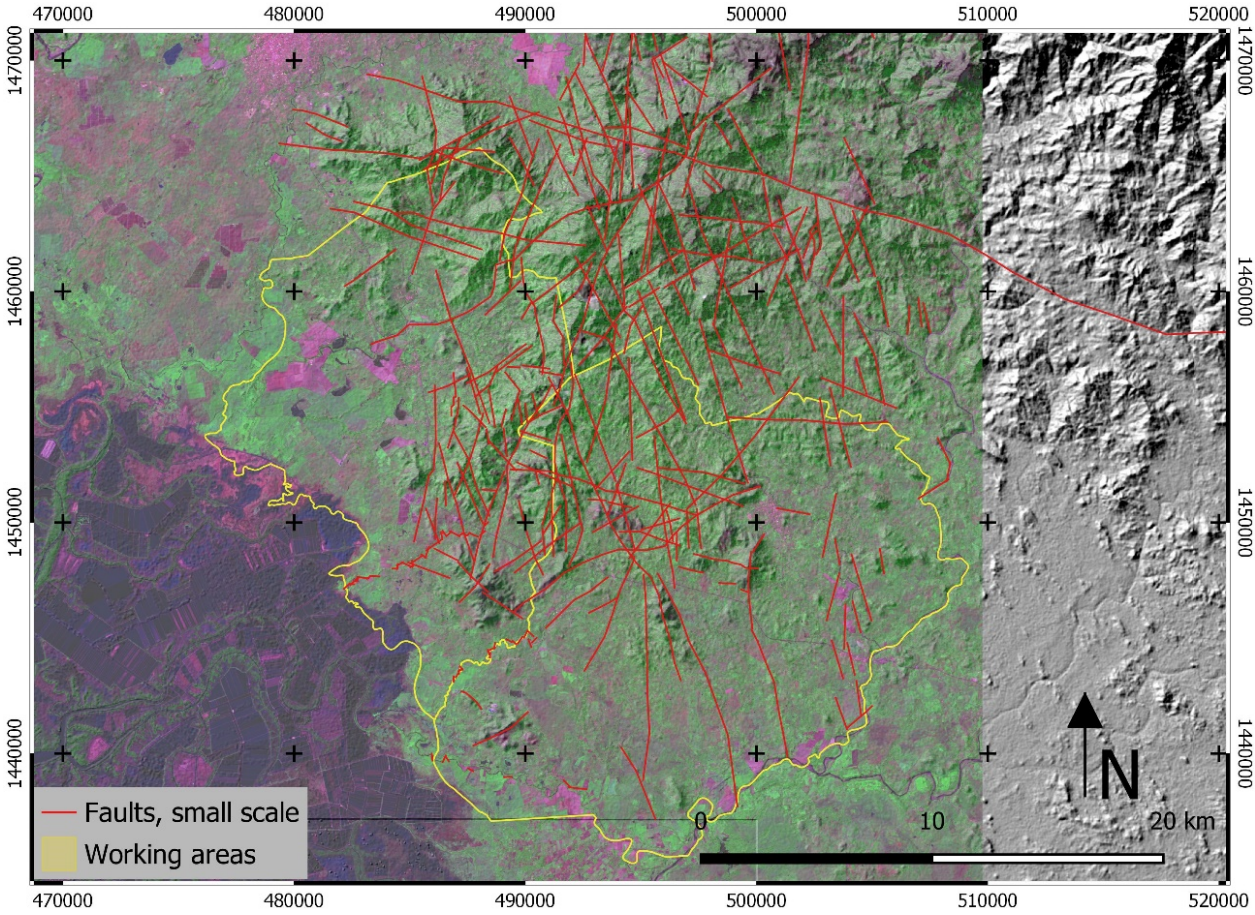

Figure 5.4: Lineaments interpreted as faults of the working areas and the surrounding areas in a small scale. Sentinel 2A, bands 12, 8a, 5 (RGB) over shaded relief SRTM DEM.

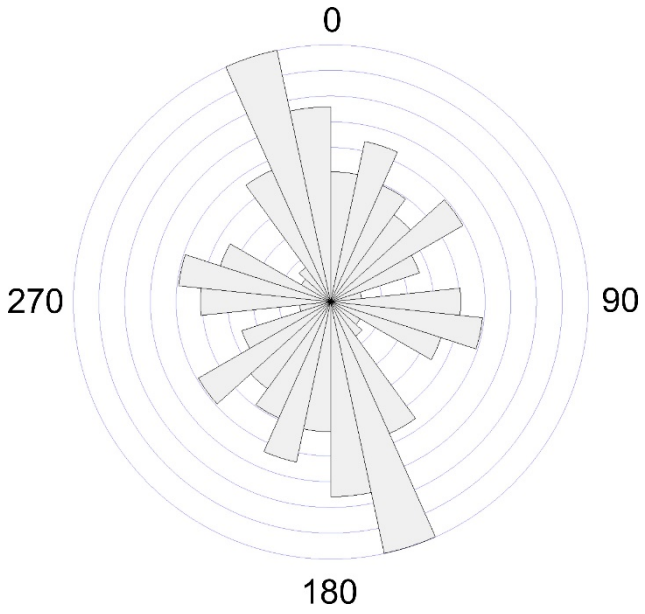

Figure 5.5: Orientations of small scale faults (n = 300) in the working areas of Namasigüe and El Trifuno (Fig.5.4) and the surrounding areas display an emphasis of NNW-SSE orientations.

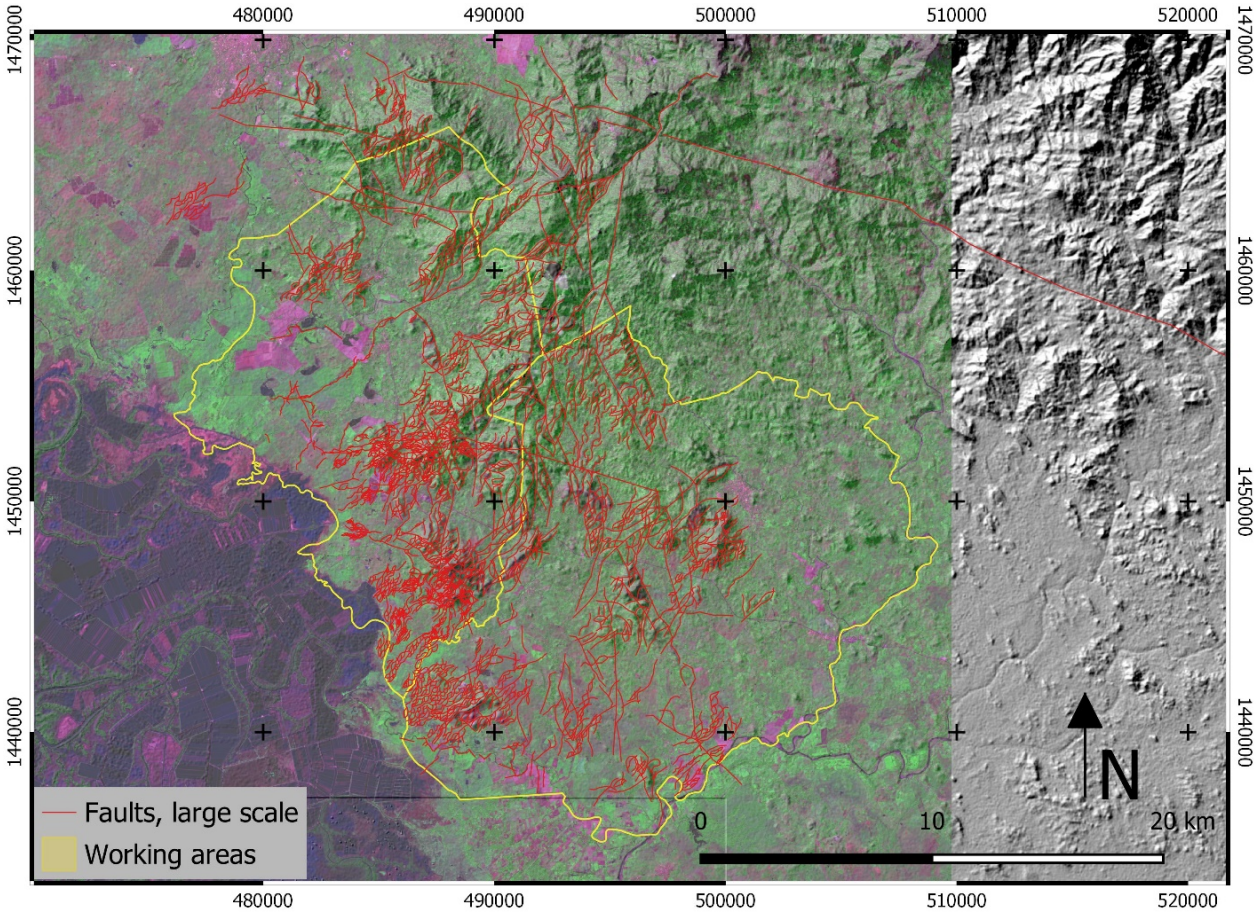

Figure 5.6: Large scale faults including the finer faults of shear lenses, of the working areas and the surrounding areas. Sentinel 2A, bands 12, 8a, 5 (RGB) over shaded relief SRTM DEM.

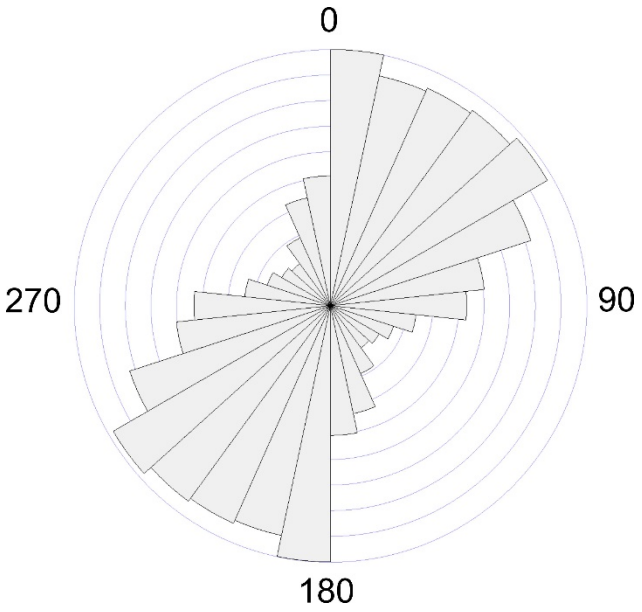

Figure 5.7: Orientations of large scale faults including the faults of shear lenses (n = 2216) in the working areas of Namasigüe and El Trifuno and the direct vicinity. The active NE-directed movement of the transtensional Guayape fault system becomes clear.

Figure 5.8: WP 012. Tear-off edges at a fault plain indicating a dextral shear sense towards 066°.

The knowledge about the kinetic sense of active tectonics together with evidence from outcrops allows to detect and interpret tectonic structures with no strong topographic expression. Shear lenses occur in the DEMs as elongated bodies and with slight differences in roughness compared to their neighbourhood. They have the same orientation and shape as well exposed shear lenses represented e.g. by ridges. Evidence for fault-bound shear lenses in topographic low areas – which are hardly visible in the field but well detectable on remote sensing data – is given by manifestations of hot springs and CO_2-degassing e.g. at the locations of waypoints 004 to 010 (Figures 5.9 to 5.12). Shear lenses occur in scales from a few metres to several kilometres.

The following examples of mapped shear lenses based on remote sensing data are more clearly visible in the GIS project layers with an appropriate scale factor than in the printed images (please refer to the attached project DVD).

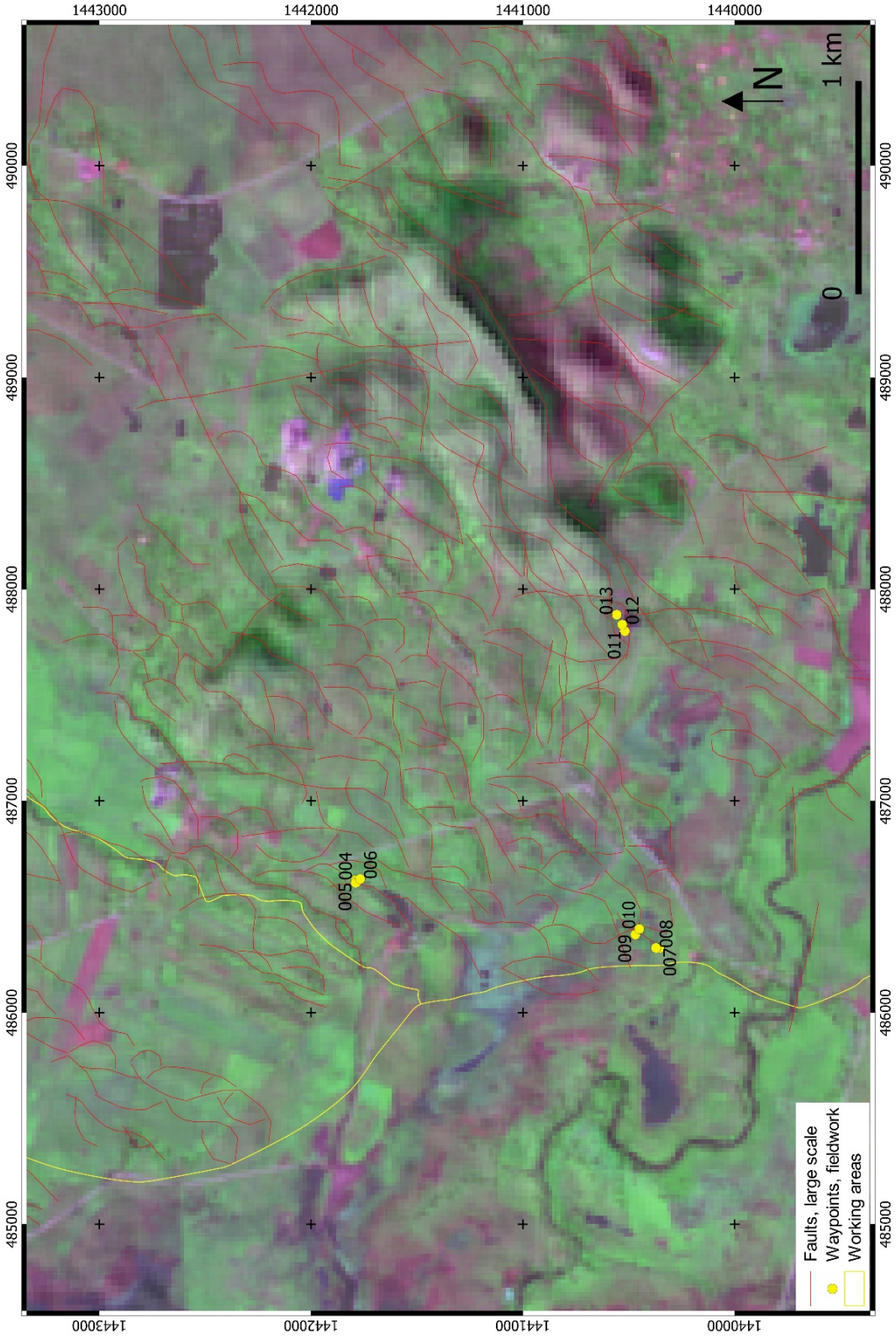

Figure 5.9: Shear lenses (delineated by fine lineaments, visible in a large scale) documented in outcrops of topographic high and low areas. At the locations of WPs 004-010 manifestations of warm and hot springs as well as CO2-degassings were found. Sentinel 2A, bands 12, 8a, 5 (RGB) over shaded relief SRTM DEM.

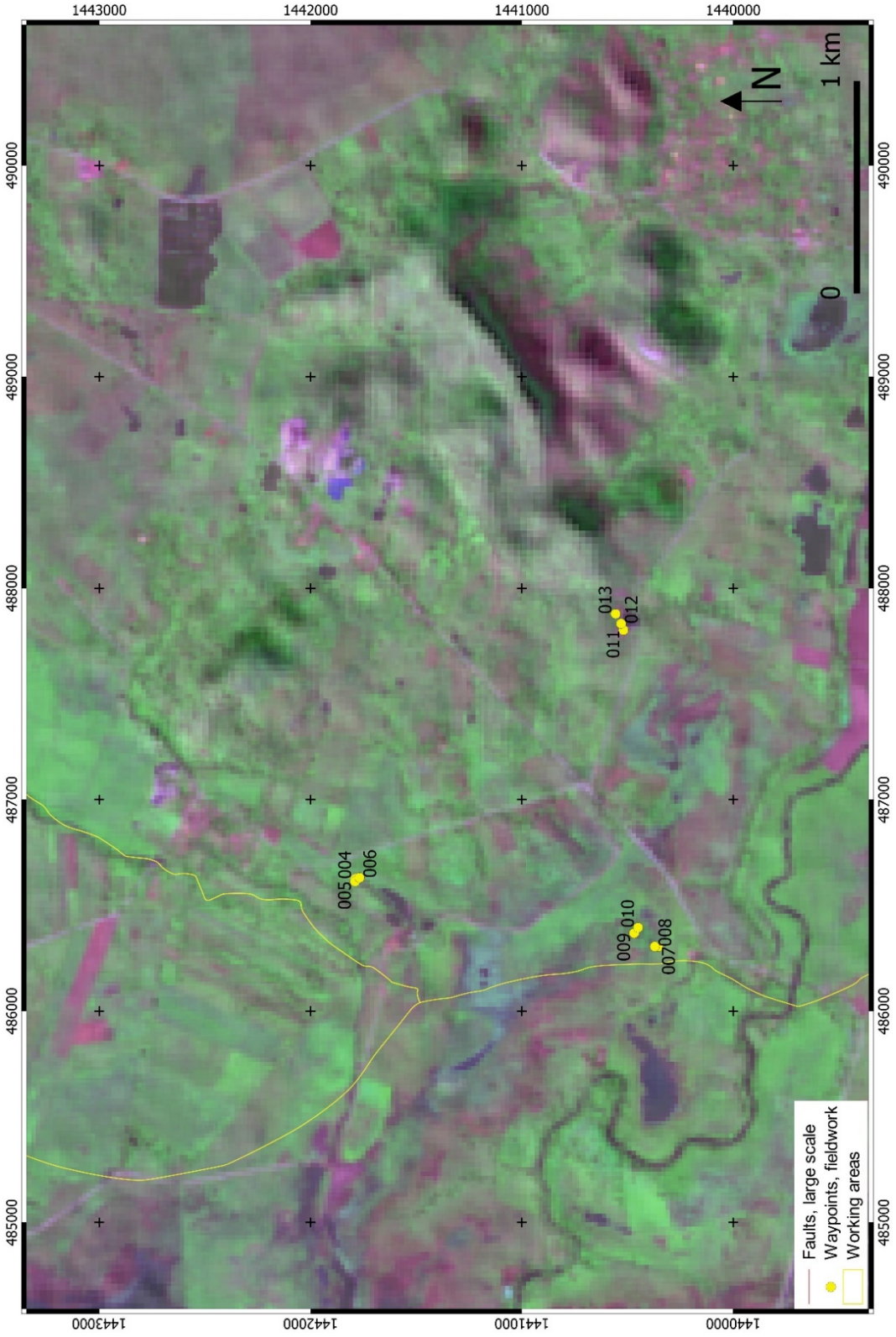

Figure 5.10: Shear lenses (not highlighted) documented in outcrops of topographic high and low areas. At the locations of WPs 004-010 manifestations of warm and hot springs as well as CO2-degassings were found. Sentinel 2A, bands 12, 8a, 5 (RGB) over shaded relief SRTM DEM.

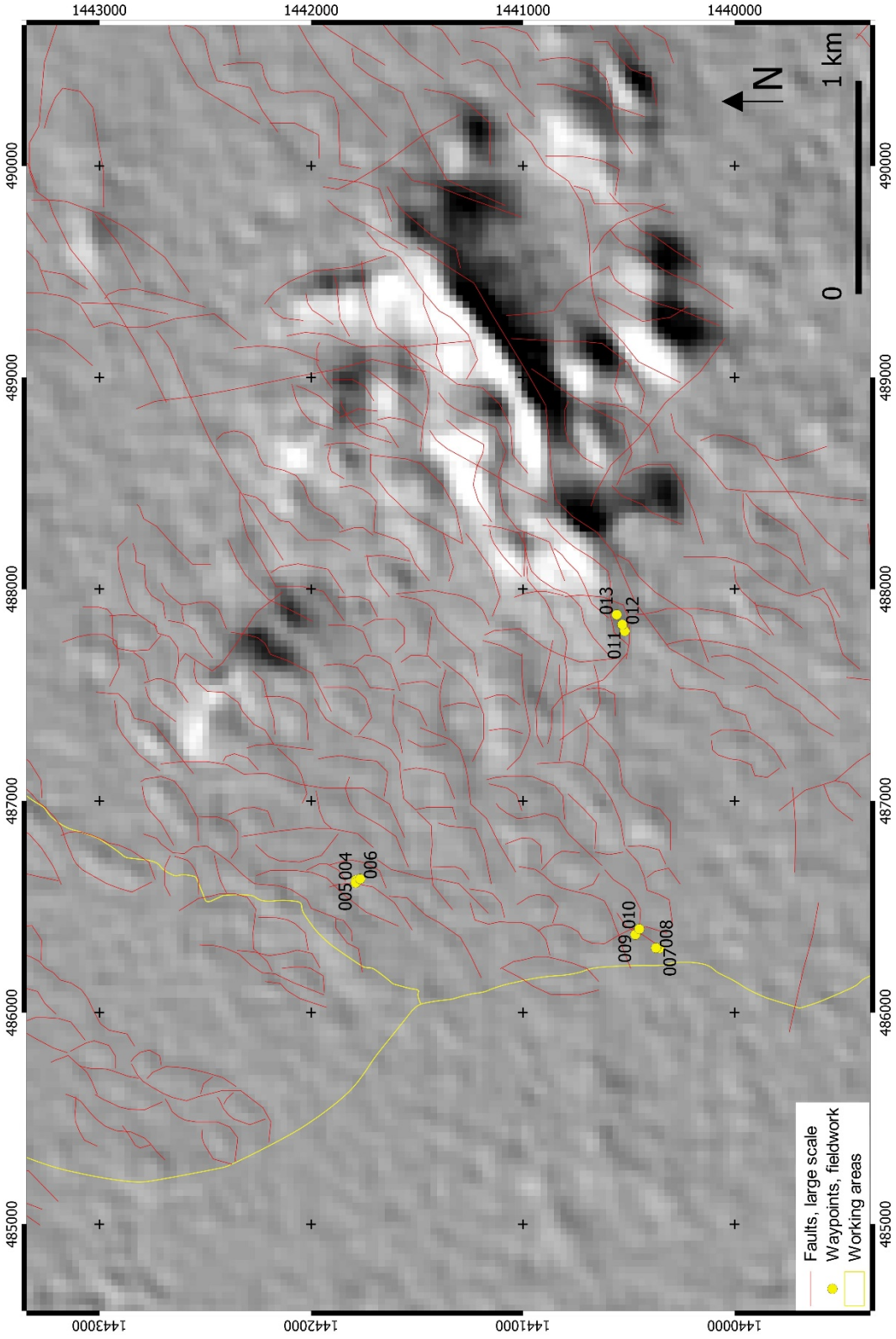

Figure 5.11: Shear lenses (delineated by fine lineaments, visible in a large scale) documented in outcrops of topographic high and low areas. At the locations of WPs 004-010 manifestations of warm and hot springs as well as CO2-degassings were found. SRTM DEM shaded relief as background.

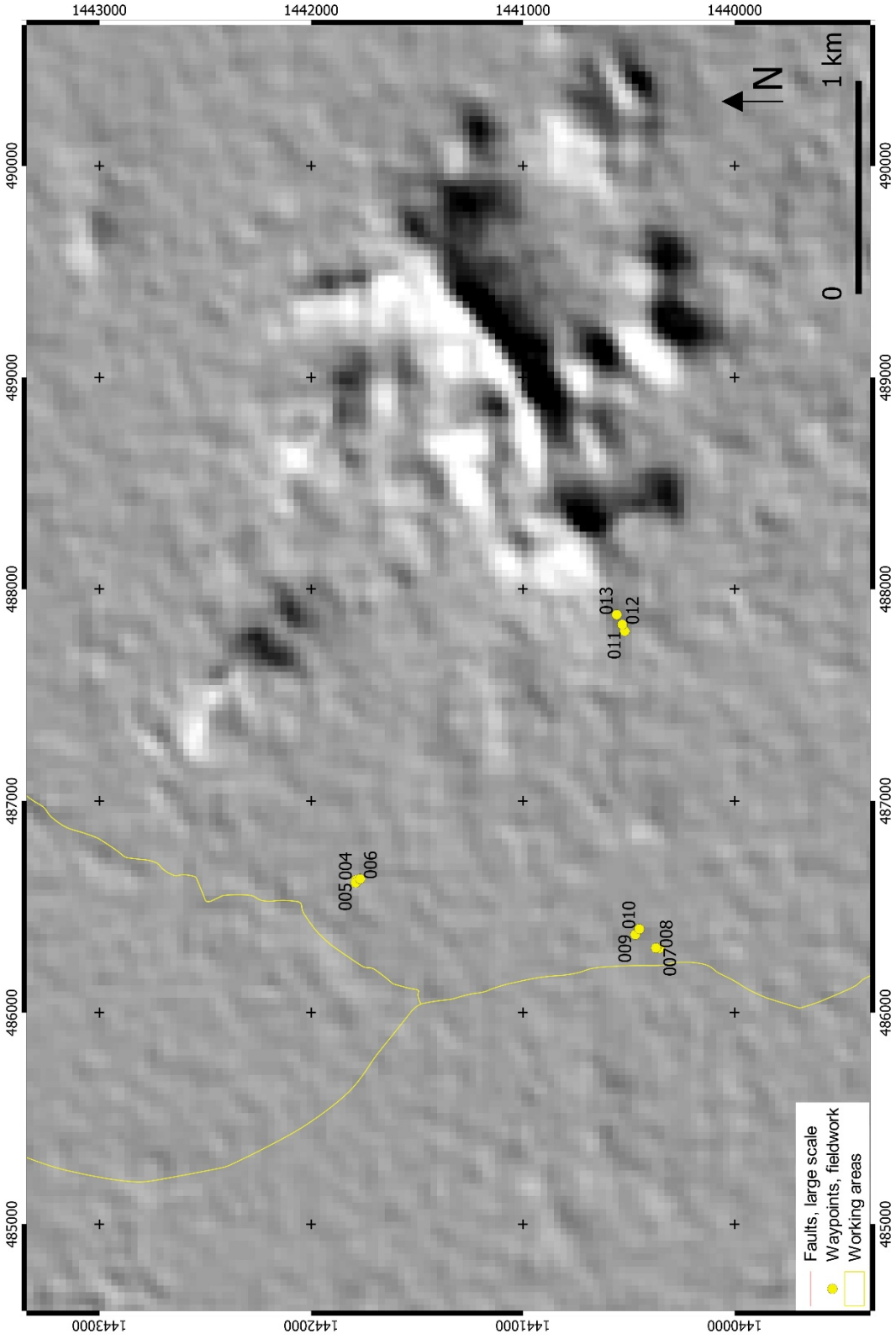

Figure 5.12: Shear lenses (not highlighted) documented in outcrops of topographic high and low areas. At the locations of WPs 004-010 manifestations of warm and hot springs as well as CO2-degassings were found. SRTM DEM shaded relief as background.

5.2 Field Work

During first field investigations, different already known manifestations were visited and measured. In addition to that, interesting lineament intersections derived through remote sensing data interpretation were investigated as well as locations where large altered areas were discovered on multispectral satellite imagery (Figure 5.16).

Manifestation 1

Location	16N 486630 1441799 (El Trifuno), WP 06.
Orientation of structures	NE-trending fault of a shear lense (Figures 5.8, 5.10).
Max. Measured Temperature	44°C
Remarks	CO_2-degassing, sulphurous precipitation. Possibly in- and outflow, but not visible.

Figure 5.13: WP 06. Manifestation 1. Large pool (min. 10 m long) 44°C warm, with sulphurous precipitations (b) and degassing (c).

Manifestations 2, 3 and 4

Location	16N 486301 1440359 (El Trifuno), WPs 08 and 07.
Structures	NE-trending fault of a shear lense
Max. Measured Temperature	71°C
Remarks	Several springs from Manifestation 2 to the NE (along a fault), with a trend to hotter temperatures to the NE. CO_2-degassing. At Manifestation 2 gas sampling was performed by BGR (B3.1) in August 2018.

Figure 5.14: WPs 08 and 07. Several manifestations along a fault with a trend to hotter temperatures to the NE.

Fault Zone 1

Location	16N 487801 1440515 (El Trifuno), WPs 011-013.
Structures	Several faults delineating shear lenses striking ENE-WSW and N-S.
Remarks	The outcropping fault plane (ca. 50 m) is part of an app. 500 m long ENE-WSW shear lense. Extensive alterations, rocks are intensely jointed, fault breccias, tear-off edges indicating right lateral shear sense (see also figure 5.8).

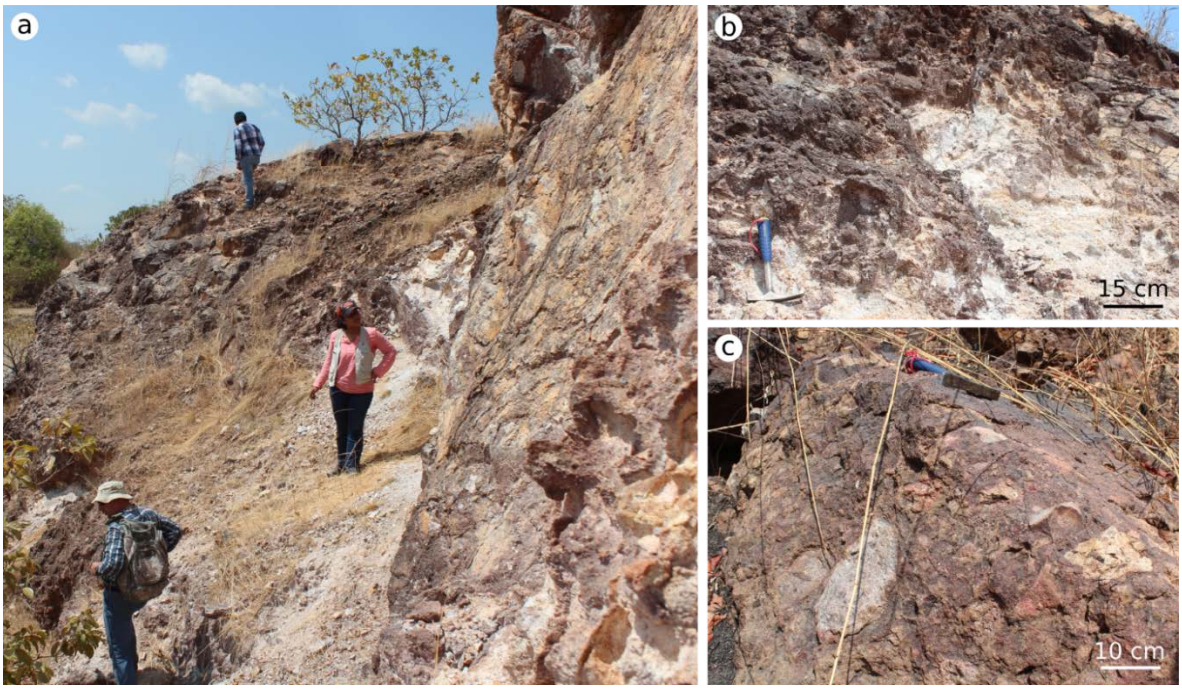

Figure 5.15: WPs 011-013. ENE-WSW fault plane (a) with extensive alterations (b) and fault breccias (c). See also figure 5.9-5.11.

Fault Zone 2

Location	16N 485540 1465808 (Namasigüe), WP 017.
Structures	Intersection of several faults with NE-, (N)W-, N- orientations.
Remarks	Large flat, altered area on a hilltop with exposed fault surface striking NW-SE. Small patch of unaltered material.

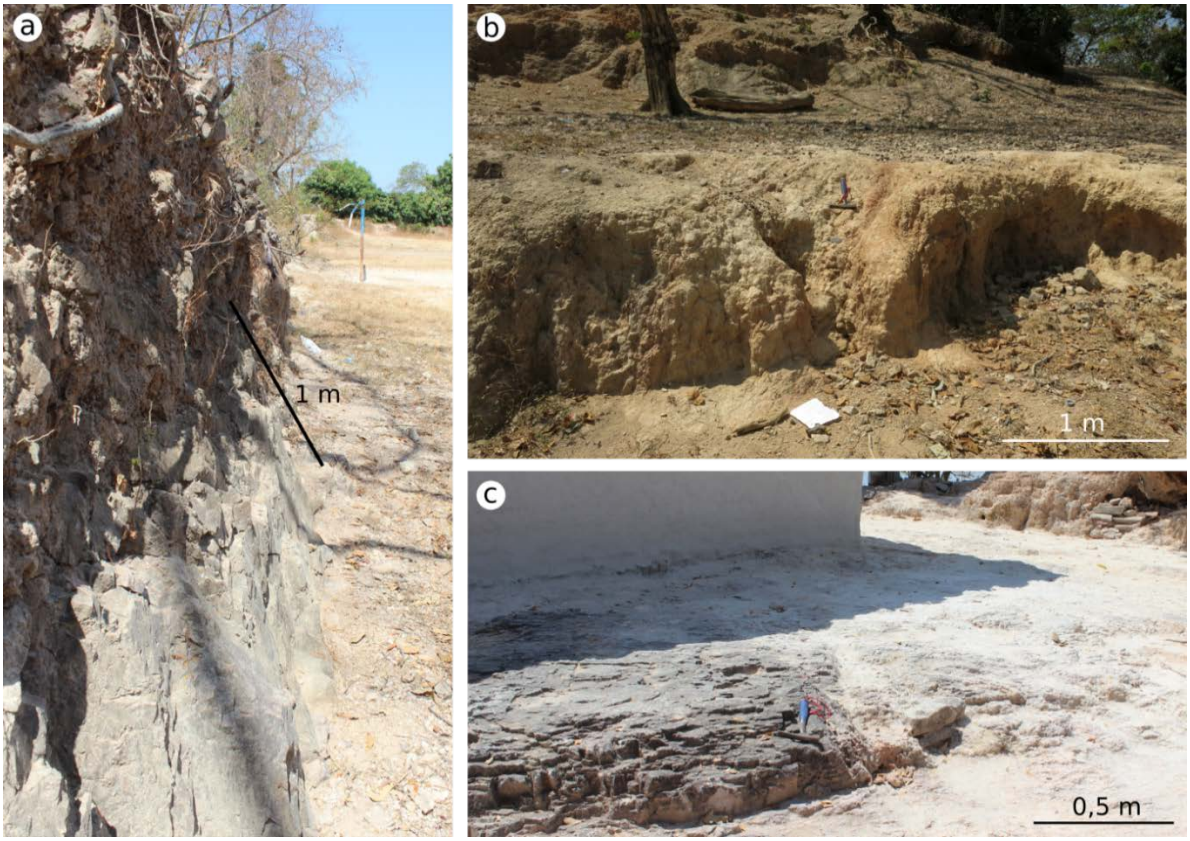

Figure 5.16: WP 017. Intersection area of several faults (a) & (b) NW-striking fault plane, (c) patch of unaltered material in an extensively altered zone.

Pavana Hot Springs

Location	16N 465509 1481293, WP 014.
Structures	NE- and NNE-striking transform faults are dominant.
Max. Measured Temperature	98°C
Remarks	Three hot springs with a diameter of ca. 30 cm - 50 cm and one fumarole, creek 1 m wide in the vicinity. Fault breccia in the area around the springs. Considered as a potential geothermal site for direct heat use (Eppler et al. 1986).

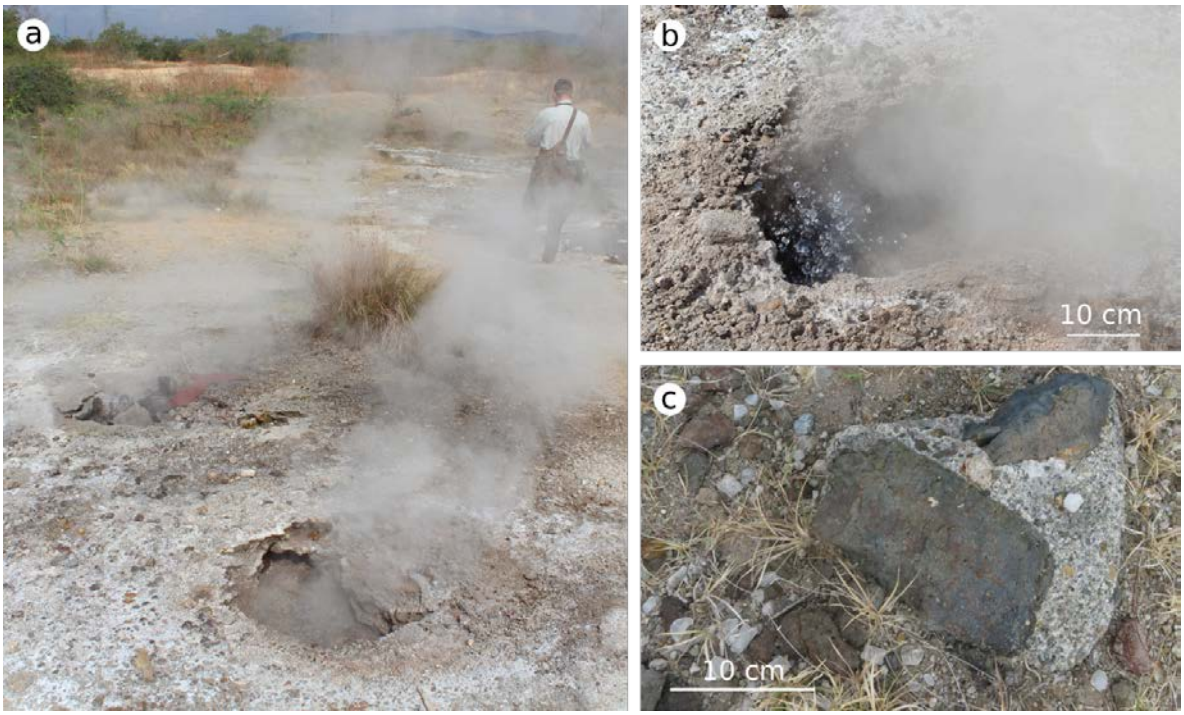

Figure 5.17: WP 014. Pavana hot springs with springs and fumaroles (a & b). Fault breccia in the area (c).

6 Conclusion and recommendation

NE-SW striking faults connected to the Guayape fault system seem to be the most active in the area by this time. These orientations occur in the working areas mainly along shear lenses, which can be detected also in topographic low areas using remote sensing data.

All visited manifestations like hot springs, degassing as well as hydrothermal alterations occur mainly along NE-SW oriented transform faults.

For a first approach, we recommend to explore areas for possible new thermal anomalies along NE-faults delineating shear lenses at locations, which carry open groundwater like in the western parts of the working areas. The presence of groundwater would especially facilitate a terrestrial survey by visual features like steam and degassing.

The usage of an UAV operating with a thermal infrared camera would simplify and speed up a survey enormously. Additionally, a thermal infrared survey should be able to also detect anomalies in areas without groundwater. Using an UAV with a high ground resolution (1 m or less) might detect thermal anomalies also adjacent to the marked faults.

It is very likely that more faults exist than being detectable in the used data sets of relatively low ground resolution. Thus, the suggested area might have additional geothermal potential neighbouring the marked fault zones.

For the first step, we suggest to focus further exploration on areas with mapped shear lenses (Figure 6.1).

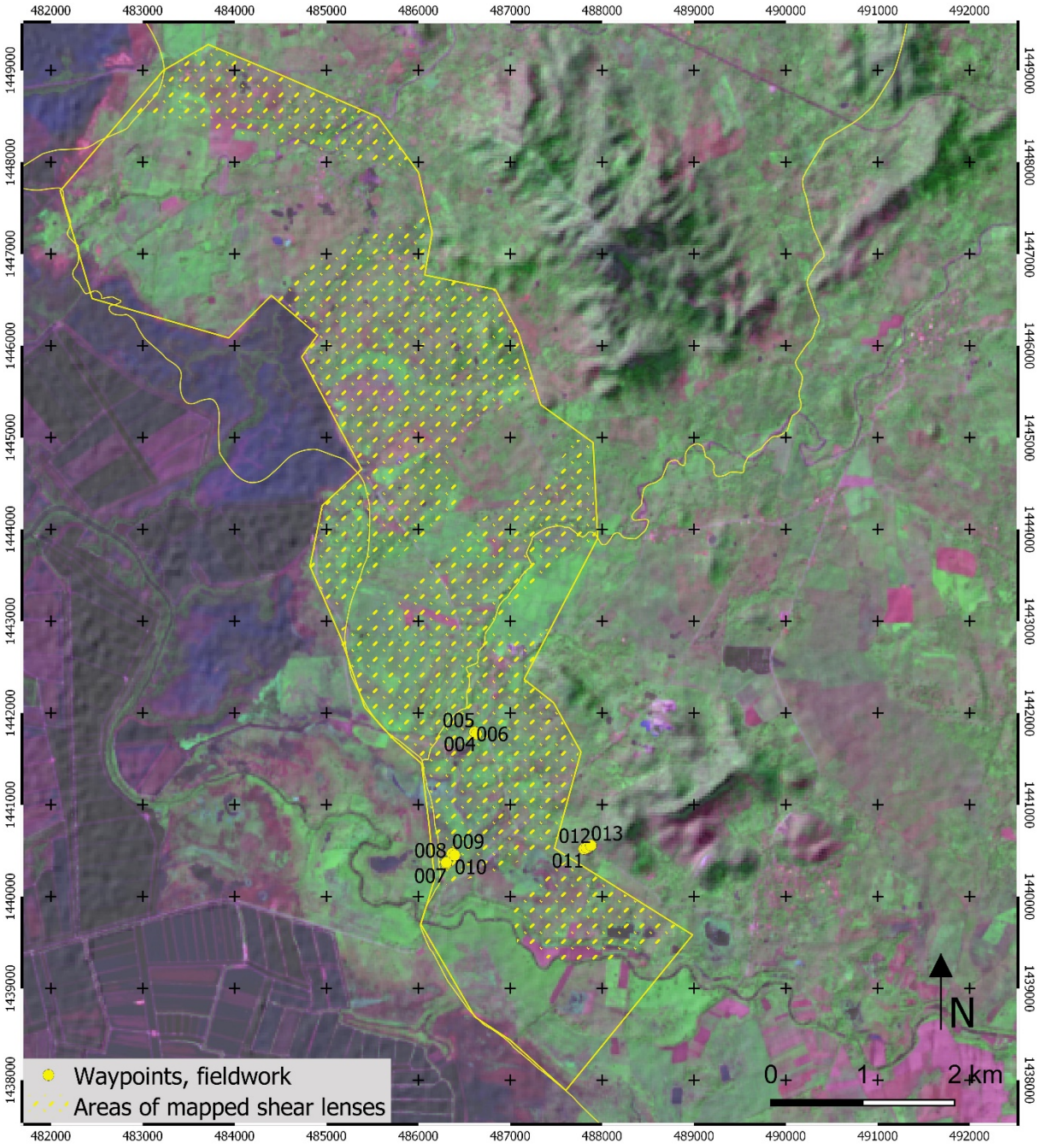

Figure 6.1: Suggested area (yellow polygon) for further geothermal exploration. Subareas of mapped shear lenses, highlighted by dashed lines, could be a preferred target. Sentinel 2A, bands 12, 8a, 5 (RGB) over shaded relief SRTM DEM.

7 References

Bundschuh, J., Winograd, M., Day, M., Alvarado, G.E. 2007. Geographical, social, economic, and environmental framework and development. *In* Bundschuh, J., Alvarado, G.E. (Eds.) *Central America: geology, resources and hazards*, *volume 1*, 75-121.

Burkart, B., & Self, S. 1985. Extension and rotation of crustal blocks in northern Central America and effect on the volcanic arc. *Geology*, *13*(1), 22-26.

DeMets, C. 2001. A new estimate for present-day Cocos-Caribbean plate motion: Implications for slip along the Central American volcanic arc. *Geophysical research letters*, *28*(21), 4043-4046.

Eppler, D., Fakundiny, R., Ritchie, A. 1986. Reconnaissance evaluation of Honduran geothermal sites. Una evaluacion por medio de reconocimiento de seis areas geotermicas en Honduras. *Los Alamos National Laboratory*, Report LA-10685-MS, UC-66b.

ESA. 2012. Sentinel-2: ESA's Optical High-Resolution Mission for GMES Operational Services (ESA SP-1322/2 March 2012). ESA Communications, Noordwijk.

Finch, R. C., & Ritchie, A. W. 1991. The Guayape fault system, Honduras, Central America. *Journal of South American Earth Sciences*, *4*(1-2), 43-60.

Frischbutter, A. 2002. Structure of the Managua graben, Nicaragua, from remote sensing images. *Geofísica Internacional*, *41*(2), 87-102.

Funk, J., Mann, P., McIntosh, K., Stephens, J. 2009. Cenozoic tectonics of the Nicaraguan depression, Nicaragua, and Median Trough, El Salvador, based on seismic-reflection profiling and remote-sensing data. *Geological Society of America Bulletin*, *121*(11-12), 1491-1521.

Heiken, G., Ramos, N., Duffield, W., Musgrave, J., Wohletz, K., Priest, S., Aldrich, J., Flores, W., Ritchie, A., Goff, F., Eppler, D., Escobar, C. 1991. Geology of the Platanares geothermal area, Departamento de Copan, Honduras. *Journal of Volcanology and Geothermal Research*, *45*(1-2), 41-58.

James, K.H. 2007. Structural geology: From local elements to regional synthesis. *In* Bundschuh, J., Alvarado, G.E. (Eds.) *Central America: geology, resources and hazards*, *volume 1*, 277-321.

La Femina, P.C., Dixon, T.H., Strauch, W. 2002. Bookshelf faulting in Nicaragua. *Geology*, *30*(8), 751-754.

Mann, P. 2007. Overview of the tectonic history of northern Central America. *In* Mann, P. (Ed) *Geologic and tectonic development of the Caribbean plate boundary in northern Central America*. Geological Society of America Special Paper 428, 1-19, doi: 10.1130/2007.2428(01)

Marshall, J.S. 2007. Geomorphology and physiographic provinces. *In* Bundschuh, J., Alvarado, G.E. (Eds.) *Central America: geology, resources and hazards*, *volume 1*, 75 - 122.

Ortega-Gutierrez, F., Solari, L.A., Ortega-Obregón, C., Elías-Herrera, M., Martens, U., Morán-Icál, S., Chiquín, M., Keppie, J.D., Torres De León, F., Schaaf, P. 2007. The Maya-Chortís boundary: a tectonostratigraphic approach. *International Geology Review*, *49*(11), 996-1024.

Ratschbacher, L., Franz, L., Min, M., Bachmann, R., Martens, U., Stanek, K., Stübner, K., Nelson, B.K., Herrmann, U., Weber, B., López-Martínez, M., Jonckheere, R., Sperner, B., Tichomirowa, M., McWilliams, M.O., Gordon, M., Meschede, M., Bock, P. 2009. The North American-Caribbean plate boundary in Mexico-Guatemala-Honduras. *Geological Society, London, Special Publications*, *328*(1), 219-293.

Rogers, R.D., Mann, P., Emmet, P.A. 2007. Tectonic terranes of the Chortis block based on integration of regional aeromagnetic and geologic data. *In* Mann, P. (Ed) *Geologic and tectonic development of the Caribbean plate boundary in northern Central America*. Geological Society of America Special Paper 428, 65 - 88 doi: 10.1130/2007.2428(04)

Swanson, M.T. 2006. Late Paleozoic strike-slip faults and related vein arrays of Cape Elizabeth, Maine. *Journal of Structural Geology*, *28*(3), 456-473.

Weinberg, R.F. 1992. Neotectonic development of western Nicaragua. *Tectonics*, *11*(5), 1010-1017.

Appendix

Waypoints of measurements and field photos as mentioned in figures. The datum of the coordinates (Decimal degrees and UTM zone 16N) is WGS84.

WP No	Lat	Lon	UTM lon	UTM lat	Altitude [m asl]	Date [yyyymmdd]
004	13.0420430	-87.1233550	486625.46	1441788.36	17.1	20190216
005	13.0420560	-87.1234720	486612.78	1441789.80	17.0	20190216
006	13.0418620	-87.1233050	486630.87	1441768.34	17.6	20190216
007	13.0290770	-87.1263140	486303.92	1440354.65	16.8	20190216
008	13.0292280	-87.1263030	486305.13	1440371.34	18.4	20190216
009	13.0301110	-87.1257220	486368.17	1440468.96	18.8	20190216
010	13.0299410	-87.1254750	486394.94	1440450.15	18.8	20190216
011	13.0305690	-87.1125030	487801.51	1440518.94	22.6	20190216
012	13.0306750	-87.1122160	487832.63	1440530.65	26.4	20190216
013	13.0309100	-87.1117880	487879.05	1440556.61	35.3	20190216
014	13.3992020	-87.3186010	465506.37	1481304.88	39.7	20190217
015	13.3991140	-87.3185020	465517.07	1481295.13	37.6	20190217
016	13.2708900	-87.1380470	485046.38	1467096.88	303.8	20190218
017	13.2594320	-87.1332430	485566.09	1465829.47	534.2	20190218
018	13.2597310	-87.1328450	485609.22	1465862.51	537.8	20190218
019	13.2591900	-87.1334420	485544.52	1465802.72	555.4	20190218
020	13.2643790	-87.1343850	485442.68	1466376.62	441.0	20190218
021	13.2733570	-87.1419380	484625.06	1467369.94	214.2	20190218
022	13.2734000	-87.1424480	484569.81	1467374.72	206.4	20190218
023	13.2734020	-87.1428160	484529.95	1467374.97	200.0	20190218
024	13.2723830	-87.1445690	484340.00	1467262.39	159.2	20190218
025	13.2777070	-87.1551520	483193.99	1467851.85	99.4	20190218
026	13.2822410	-87.1641920	482215.11	1468353.89	88.0	20190218
027	13.2842730	-87.1669330	481918.36	1468578.80	75.0	20190218
028	13.3591300	-87.2788350	469806.71	1476868.08	99.1	20190219
029	13.3549270	-87.2699650	470766.69	1476402.21	96.6	20190219
030	13.3470330	-87.2586280	471993.42	1475527.90	76.4	20190219

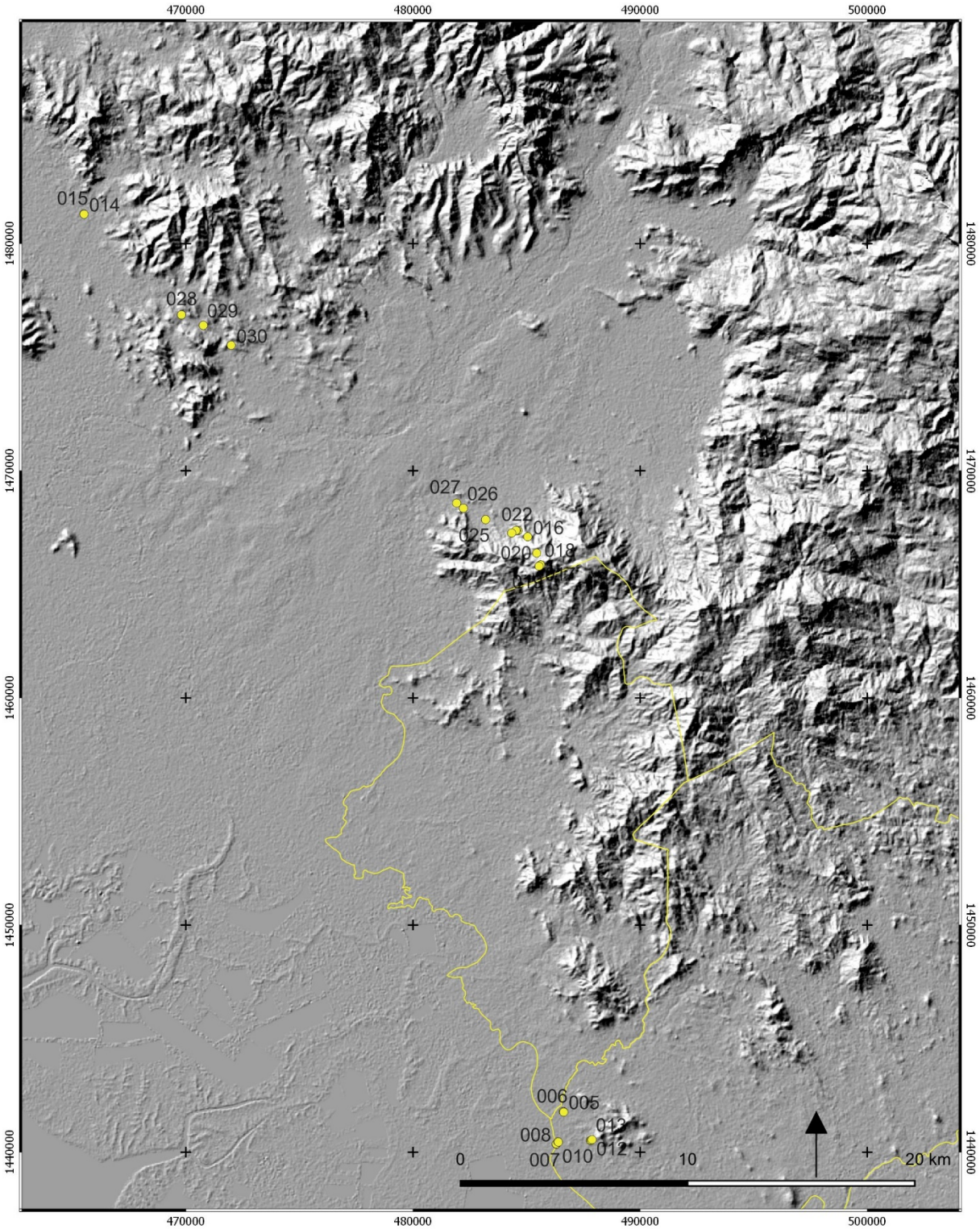

Waypoints with numbers (as referred to in figures) of the working areas projected into SRTM shaded relief elevation model.